

# Suprachoroidal Electrotransfer: A Nonviral Gene Delivery Method to Transfect the Choroid and the Retina Without Detaching the Retina

Elodie Touchard<sup>1-3</sup>, Marianne Berdugo<sup>1-3</sup>, Pascal Bigey<sup>4-7</sup>, Mohamed El Sanharawi<sup>1-3</sup>, Michèle Savoldelli<sup>8</sup>, Marie-Christine Naud<sup>1-3</sup>, Jean-Claude Jeanny<sup>1-3</sup> and Francine Behar-Cohen<sup>1-3,8</sup>

<sup>1</sup>INSERM, U872 Physiopathology of Ocular Diseases: Therapeutic Innovations, Paris, France; <sup>2</sup>Centre de Recherche des Cordeliers, Université Pierre et Marie Curie—Paris6, UMR S 872, Paris, France; <sup>3</sup>Université Paris Descartes, UMR S 872, Paris, France; <sup>4</sup>INSERM, U640, Paris, France; <sup>5</sup>CNRS, UMR8151, Paris, France; <sup>6</sup>Chemical and Genetic Pharmacology Laboratory, Faculté de Pharmacie, Université Paris Descartes, Paris, France; <sup>7</sup>ENSCP Chimie ParisTech, Paris, France; <sup>8</sup>Department of Ophthalmology, Hôtel-Dieu de Paris, Paris, France

Photoreceptors and retinal pigment epithelial cells (RPE) targeting remains challenging in ocular gene therapy. Viral gene transfer, the only method having reached clinical evaluation, still raises safety concerns when administered via subretinal injections. We have developed a novel transfection method in the adult rat, called suprachoroidal electrotransfer (ET), combining the administration of nonviral plasmid DNA into the suprachoroidal space with the application of an electrical field. Optimization of injection, electrical parameters and external electrodes geometry using a reporter plasmid, resulted in a large area of transfected tissues. Not only choroidal cells but also RPE, and potentially photoreceptors, were efficiently transduced for at least a month when using a cytomegalovirus (CMV) promoter. No ocular complications were recorded by angiographic, electroretinographic, and histological analyses, demonstrating that under selected conditions the procedure is devoid of side effects on the retina or the vasculature integrity. Moreover, a significant inhibition of laser induced-choroidal neovascularization (CNV) was achieved 15 days after transfection of a soluble vascular endothelial growth factor receptor-1 (sFlt-1)-encoding plasmid. This is the first nonviral gene transfer technique that is efficient for RPE targeting without inducing retinal detachment. This novel minimally invasive nonviral gene therapy method may open new prospects for human retinal therapies.

Received 4 April 2011; accepted 18 December 2011; advance online publication 17 January 2012. doi:10.1038/mt.2011.304

## INTRODUCTION

Because the eye is a small, confined organ, isolated by barriers, it has been identified as an organ of choice for local gene therapy. On the other hand, hereditary retinal dystrophies inducing blindness in >1.5 million people over the world are due to mutations in genes encoding proteins in photoreceptors (cones and rods) or in

retinal pigment epithelial cells (RPE).<sup>1</sup> Whilst gene replacement in photoreceptor cells is still under preclinical evaluation, striking advances have been made for gene replacement in RPE cells of patients with Leber congenital amaurosis. Using viral vectors, not only RPE65 gene transfer in the RPE was shown efficient in animal models,<sup>2,3</sup> but recently, patients have received the subretinal injection of recombinant adeno-associated viral vector 2 with promising functional results,<sup>4-6</sup> raising new hopes for patients suffering from inherited blinding diseases.

Subretinal injections of viral vectors have been shown to efficiently transfect RPE cells and photoreceptors and have served to validate the first proof-of-concepts.<sup>7</sup> However, injection of therapeutic vectors into the subretinal space continues to raise safety concerns. Indeed, RPE cells and photoreceptors are only transfected in, and at the vicinity of the detached retina area, which implies detaching the macula if central vision recovery is targeted, potentially threatening visual recovery.<sup>8-10</sup> Safety studies in nonhuman primates have shown that subretinal injections could induce an abnormal architecture of the fovea<sup>11</sup> and two independent gene therapy clinical trials have highlighted the risk of developing a macular hole<sup>6</sup> or a foveal thinning<sup>5</sup> after subretinal administration of vector. The exact consequences of macular detachment in patients with retinal dystrophies are not yet known. However, patients with resolved transitory spontaneous serous retinal detachment due to central serous chorioretinopathy had a decrease in the central foveal thickness in the involved eyes, and there was a statistically significant correlation between the foveal thickness and the visual acuity, even in eyes with relatively good visual acuity,<sup>12</sup> suggesting that even without any iatrogenic manipulation, transitory sub macular detachment may alter the foveal function. Moreover, even if controversies still exist regarding the factors that may predict visual recovery after macular detachment in the case of rhegmatogenous detachment, the health of the macula at the time of reattachment is probably the most critical variable.<sup>13</sup> Because uncertainty still exists regarding central vision recovery after sub macular injection in diseased eyes, the development of transfection techniques that would achieve to transfect

The first two authors contributed equally to the work.

Correspondence: Francine Behar-Cohen, Centre de Recherche des Cordeliers UMR S 872 Equipe 17, 15 rue de l'École de Médecine 75 006 Paris, France. E-mail: francine.behar-cohen@crc.jussieu.fr

RPE cells without any surgical detachment of the retina would be a gain for retinal safety.

Many nonviral gene transfer vectors or methods have been developed and adapted for ocular gene therapy<sup>14–16</sup> to circumvent the putative safety concerns associated with the subretinal administration of viral vectors such as the long-term persistence of viral particles into the retina and the brain.<sup>8,10</sup> Electroporation, also called electrotransfer (ET) when the electrical field drives plasmid DNA into cells, has been widely used in many cells and tissues and was shown to be amongst the more efficient both in preclinical<sup>17–19</sup> or clinical studies.<sup>20</sup> In the field of ocular gene therapy, previous reports have shown that after subretinal administration of plasmids, ET allowed the efficient transfection of new-born murine RPE and photoreceptor cells<sup>21</sup> and delayed retinal degeneration in animal models.<sup>22</sup> Efficient and prolonged RPE transfection was also achieved in the adult rat after ET of subretinal plasmids containing specific RPE promoters.<sup>23</sup> However, to date, only viral vectors have reached the clinical evaluation.

Our team has been the first investigating the feasibility and tolerance of suprachoroidal injection, consisting in injection into the suprachoroidal space,<sup>24</sup> and the tolerance of this approach has then been validated in the macula region.<sup>25</sup> The aim of this study

was to evaluate whether suprachoroidal injection of a plasmid solution in the rat eye, associated with extraocular electroporation could be efficient for the transfection of the choroid and the retina. We bring here the first proof of concept that using this minimally invasive technique, that do not require subretinal injection and retinal detachment, choroidal cells, RPE cells but also photoreceptors can be efficiently transfected.

## RESULTS

### Suprachoroidal injection

To validate injections into the suprachoroidal space, *i.e.*, between the sclera and the underlying choroid (Figure 1a), the procedure was first monitored *in vivo* using Mayer's hemalun solution ( $n = 5$ ). Diffusion of the dye into the suprachoroidal space during injection could be visualized in real time from the external side of eyes from albino rats. When the injection needle was removed after the injection was over, a colored circle area corresponding to the putative area of suprachoroidal pocket could be observed from outside the eye (Figure 1b). No subretinal bleb, corresponding to a detachment between photoreceptor outer segments (OS) and RPE could be noticed on eye fundus, the dye being localized deeper into the suprachoroidal space (Figure 1c). To confirm

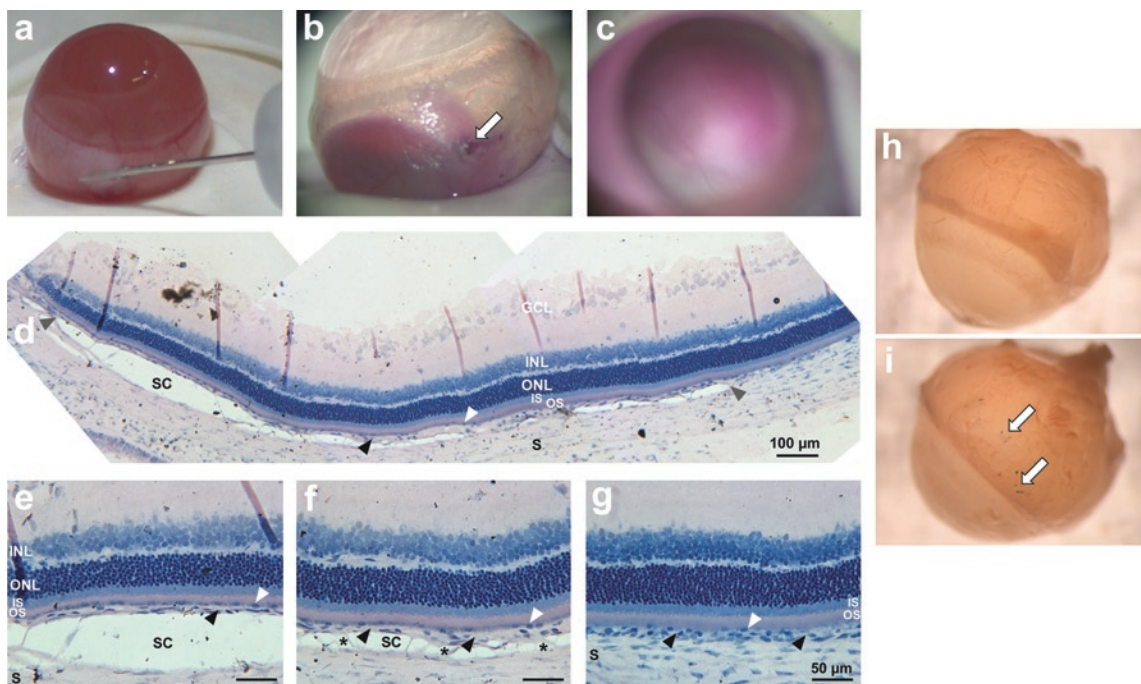


**Figure 1** Suprachoroidal injection technique in the rat eye. **(a)** Surgical procedure of solution (plasmid DNA, vehicle or dye) injection in the suprachoroidal space using a 30G injection needle. **(b)** Mayer's hemalun solution (dye) visualized macroscopically from outside the eye immediately after injection needle withdrawal ( $n = 5$ ). The needle insertion site is visible on the eye surface (white arrow). **(c)** Eye fundus observed immediately after injection of Mayer's hemalun solution showing suprachoroidal localization of the dye, with no subretinal bleb formation. **(d–g)** Resin histological section of an eye fixed a few minutes after injection and stained with toluidin blue ( $n = 5$ ). A suprachoroidal detachment (SC), delineated by gray arrowheads, is observed in the half anterior part of the retina **(d)**. Detachment is observed between the sclera (S) and the underlying choroid (black arrowheads) **(d–f)**, whereas the choroid/choriocapillary (black arrowheads) still adheres to the retinal pigment epithelial (RPE) cell layer (white arrowheads). The detachment is thinner in the posterior and medium part of the detachment bleb **(f)** than in the anterior part **(e)**, with focal connections between the choroid and the sclera (asterisks). No detachment is induced between the RPE cells and photoreceptor outer segments (OS) (*i.e.*, no subretinal detachment) and no folding of the neuroretina, containing the ganglion cell layer (GCL), the inner nuclear layer (INL), the outer nuclear layer (ONL), and the photoreceptor inner (IS)/outer (OS) segments, is induced. No bleeding is observed around choriocapillary/choroid vessels. Outside of the detachment area, the choroid adheres to the sclera **(g)**, as observed in untreated eyes (data not shown). **(h, i)** LacZ reporter gene expression (blue coloration indicated by white arrows) visualized from outside the eye, 7 days after injection of 30  $\mu$ g (in 30  $\mu$ l) of **(h)** pVAX1 or **(i)** pVAX1-LacZ ( $n = 4$  eyes/group).

these macroscopic observations, resin histological sections were performed on the same eyes fixed a few minutes after the injection. A detachment between the choroid and the sclera could be highlighted in the five eyes analyzed, keeping the whole neural retina adherent to retinal pigment epithelial (RPE) cells that still adhered to bruch's membrane and choriocapillary/choroid (**Figure 1d–g**). The detachment spread on the half anterior part of the temporal hemisphere (**Figure 1d**). It was large and complete in the anterior part, next to the needle insertion site (**Figure 1e**), and progressively decreased posteriorly, with apparent focal attachments between the choroid and the sclera (**Figure 1f**). Observations made posteriorly to the suprachoroidal detachment showed that the choroid was in close contact with the sclera (**Figure 1g**), as observed in untreated control eyes (data not shown). In all of the following experiments, eye fundus examination was performed after the injection to exclude from the analysis eyes with bleb of retinal detachment. Only two eyes among all treated eyes were excluded from the analysis because of accidental subretinal injection. Note that no bleeding or hemorrhage were noticed in any of the eyes during (**Figure 1a**) or immediately after the surgery (**Figure 1b–g**), nor 7 days (**Figure 1i**) after injection alone.

Very faint or no  $\beta$ -galactosidase activity was observed 7 days after the simple suprachoroidal injection of pVAX1-LacZ plasmid DNA (**Figure 1i**) and no blue coloration was found with the pVAX1 plasmid backbone (**Figure 1h**), demonstrating that no or very poor transfection occurs with injection alone ( $n = 4$ /group).

### Electrical devices for suprachoroidal ET

Immediately after plasmid injection (30  $\mu$ g in 30  $\mu$ l of pVAX1-LacZ) in the suprachoroidal space, the injected area was submitted to an electric field (ET procedure), created by the application of

different electrode shape and placement. The electric field of 40V/cm intensity was created using 8 pulses of 20V voltage intensity and 20ms duration, with a frequency of 5 Hz. Compared to injection alone (**Figure 1i**),  $\beta$ -galactosidase gene expression was significantly enhanced by ET with all the tested electrodes. However, each device exhibited different transfection efficacy. In preliminary experiments, the device used was the one that has been developed in our laboratory to transduce ocular ciliary muscle fibers *in vivo* by ET,<sup>26</sup> with some adaptations regarding the positioning of both electrodes. A platinum/iridium (Pt/Ir) wire (250  $\mu$ m in diameter, negative pole) was inserted into the suprachoroidal space, after the needle of injection was withdrawn, facing a semiannular Pt/Ir sheet (anode electrode) attached to the sclera at the opposing side of the injection site ( $n = 4$ ). In such conditions, the area of tissue expressing  $\beta$ -galactosidase observed from outside the eye appeared as a line corresponding to the site where the wire electrode had been inserted (data not shown). To extend plasmid DNA cellular uptake and expression, we decided to use larger electrodes and to place them externally. When a semiannular Pt/Ir sheet (anode) was placed on the scleral surface located above the inoculated area with a semiannular Pt/Ir wire electrode (cathode) positioned on the scleral surface, at the base of the posterior pole of the eye (device 1, **Figure 2a,b**),  $\beta$ -galactosidase expression was localized in the anterior part of the posterior segment (**Figure 2c**), where the sheet electrode was located ( $n = 4$ ). When a contact curved Pt/Ir sheet (anode, +) was attached to the sclera above the injected area with a semiannular Pt/Ir sheet (cathode, -) placed on the sclera, facing the anode at the opposing side of the eye (device 2, **Figure 2d,e**), the area of tissue expressing the  $\beta$ -galactosidase reporter gene was greatly extended as compared with the two other devices (**Figure 2f**) ( $n = 4$ ). With such a device, the anode covered the whole area of

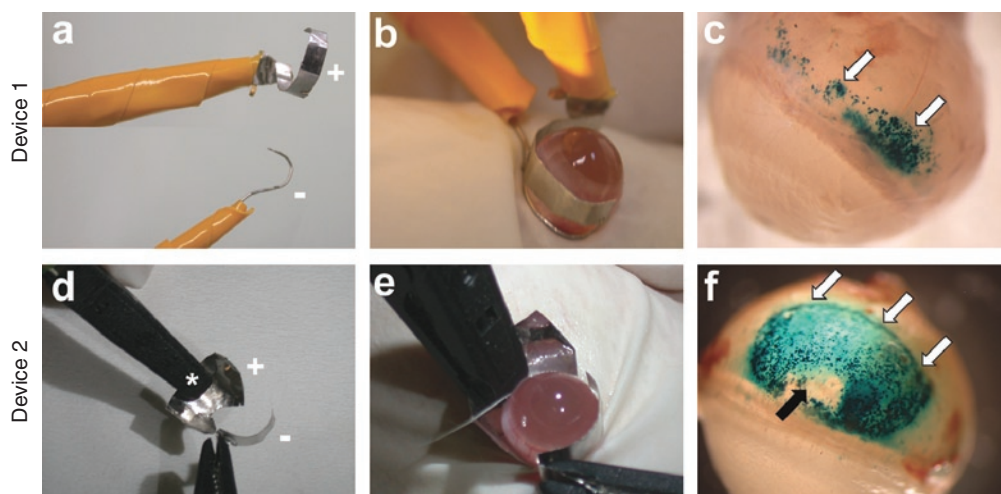


**Figure 2** Evaluation of electrical devices for suprachoroidal gene transfer electrotransfer. Injection of 30  $\mu$ g (in 30  $\mu$ l) of pVAX1-LacZ plasmid DNA, carrying the *LacZ* reporter gene, into the suprachoroidal space (**Figure 1a**) was followed by electrotransfer. Delivery of electrical pulses (8 pulses, 40V/cm, 20ms, 5 Hz) was performed using two different electrical devices. (**a,b**) Device 1 is made of a semiannular platinum/iridium sheet (anode electrode, +) placed on the scleral surface located above the inoculated area and a semiannular platinum/iridium wire electrode (cathode, -) positioned on the scleral surface, at the base of the posterior pole of the eye. (**d,e**) Device 2 is made of a contact curved platinum/iridium sheet (anode, +) attached to the sclera located above the injected area and a semiannular platinum/iridium sheet (cathode, -) placed on the sclera, facing the anode at the opposing side of the eye. (**c,e,f**) Localization of  $\beta$ -galactosidase expression (blue coloration indicated by white arrows) from outside the eye 7 days after electrotransfer (ET) pVAX1-LacZ (30  $\mu$ g in 30  $\mu$ l): the area of tissue expressing  $\beta$ -galactosidase reporter protein is more extended using device 2 than device 1 ( $n = 4$  eyes/group). In **f**, the central area exhibiting no  $\beta$ -galactosidase activity (black arrow) corresponds to the area of tissue exposed to the forceps connected to the anode (asterisk in panel **d**).

suprachoroidal detachment and reporter gene was expressed in almost the whole detached surface (Figures 1b and 2f), except for the little zone where no electrical field was generated and corresponding to the plastic connecting forceps placed on the eye surface to maintain the contact curved electrode (Figure 2f, black arrow). No blue coloration could be observed in eyes treated by ET of the pVAX1 backbone, whatever the electrical device used (data not shown, similar to that seen in Figure 1h;  $n = 4$  for each device). No hemorrhage was noticed during electrical field application or 7 days after ET (Figure 2c,f).

### Optimal electrical parameters for suprachoroidal ET

Using device 2 (Figure 2d,e) several set of electrical parameters were tested after injection of 30  $\mu\text{g}$  (in 30  $\mu\text{l}$ ) of pVAX1-LacZ into the suprachoroidal space, varying in electrical field intensity (V/cm) and pulse duration (ms) ( $n = 7$  eyes for each experimental condition). Seven days after treatment, transfection efficacy visualized by  $\beta$ -galactosidase expression (blue coloration) was not different in eyes submitted to eight pulses of 14 V/cm (20 ms, 5 Hz) (Figure 3a) than that obtained in eyes treated by injection alone (Figure 1i). On the contrary, application of eight pulses (20 ms, 5 Hz) with an electrical field intensity of 30, 60, and 120 V/cm significantly

enhanced  $\beta$ -galactosidase expression (Figure 3b–d, respectively) compared to eyes treated by injection alone. Transfection efficacy increased with increasing electrical field intensities, the better efficacy being obtained with 60 V/cm. Using this condition, reporter gene expression could be detected in almost the whole temporal hemisphere (Figure 3i). We demonstrated otherwise that reporter gene activity was as, even more, efficient using a 40 V/cm electrical field intensity (Figures 2f and 5a) than using a 60 V/cm intensity.

As judged by paraffin histological section analysis, retinal morphology was well preserved in eyes submitted to electrical fields inferior or equal to 60 V/cm (Figures 3f,g, and 4d-f) compared to control eyes treated by injection alone (Figure 3e). Indeed, retinal layers had similar organization and thicknesses in the areas transfected by means of electrical field application to that observed in areas injected only. However, application of a 120 V/cm field intensity induced a marked retinal disorganization of all retinal layers and an increase in retinal thickness maybe induced by an edema phenomenon (Figure 3h). Note that no hemorrhage could be detected 7 days after electrical field application, whatever the intensity considered. Thus, electrical field application seemed to be safe under selected conditions, at

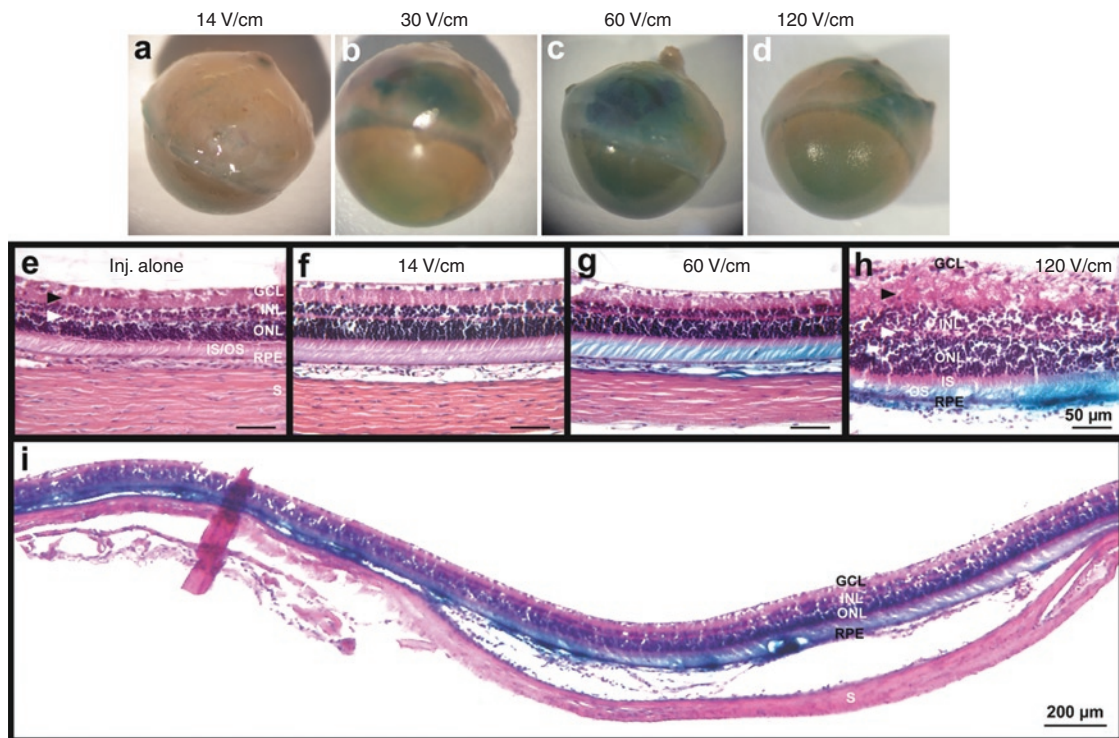


**Figure 3** Evaluation of electrical parameters for suprachoroidal gene transfer by electrotransfer. Eyes were injected with 30  $\mu\text{g}$  (in 30  $\mu\text{l}$ ) of pVAX1-LacZ plasmid DNA into the suprachoroidal space (Figure 1a) and submitted to electrotransfer using the device 2. Eight electrical pulses of 20 ms duration were applied at the frequency of 5 Hz, varying in voltage intensity. Analysis of gene expression was performed 7 days after transfection. (a–d) Extent and intensity of  $\beta$ -galactosidase expression (blue coloration) observed from outside the eye, in eyes treated by ET using electrical field intensities (voltages) of (a) 14 V/cm (7V), (b) 30 V/cm (15V), (c) 60 V/cm (30V), or (d) 120 V/cm (60V) ( $n = 4$  eyes/group). (e–i) Paraffin histological sections stained with hematoxylin and eosin from an eye treated with injection (inj.) alone (e) and from eyes treated by ET using electrical field intensities of (f) 14 V/cm, (g,i) 60 V/cm, and (h) 120 V/cm ( $n = 4$  eyes/group). Photo e–i were taken in the transfected area of the temporal hemisphere at (i) low or (e–h) higher magnification. GCL, ganglion cell layer; INL, inner nuclear layer; ONL, outer nuclear layer; IS/OS, photoreceptor inner/outer segments; RPE, retinal pigment epithelium; S, sclera. Black and white arrowheads indicated the inner and outer plexiform layers, respectively.

least to the retinal morphology point of view. Since the lowest electrical field intensity consistent with a safe and effective gene transfer was 40 V/cm, further experiments were performed using this parameter.

With respect to pulses duration, transfection efficacy was significantly higher using pulses of 20 ms than that of 10 ms (both at 40 V/cm and 60 V/cm, data not shown,  $n = 4$  eyes/group), explaining why this duration has been chosen in further experiments.

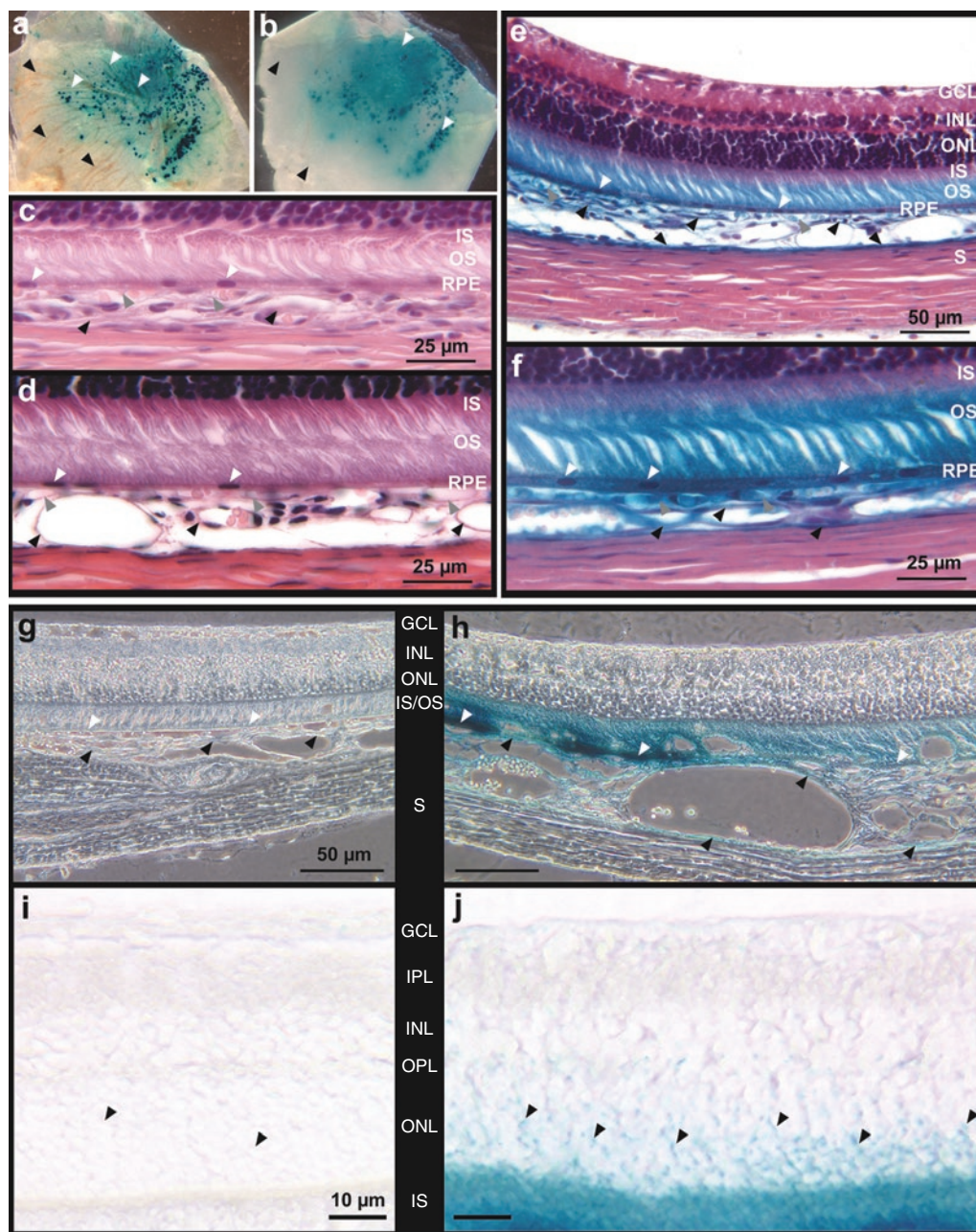


**Figure 4** Localization of *LacZ* gene expression. Eyes were injected with 30  $\mu$ g (in 30  $\mu$ l) of pVAX1-*LacZ* plasmid DNA into the suprachoroidal space (**Figure 1a**) and submitted to electrotransfer (eight pulses, 40V/cm, 20ms, 5 Hz) using the device 2 (**Figure 2d,e**). Analysis of gene expression was performed 7 days after transfection. (**a,b**) Flatmount of a (**a**) RPE–choroid–sclera complex and the (**b**) corresponding neuroretina showing transfection in the temporal hemisphere. Photos are taken from the RPE side (**a**) and from the photoreceptor outer segment side (**b**). White arrowheads point out vessels (**a**) and neuronal tissue areas (**b**) expressing the  $\beta$ -galactosidase enzyme in the transfected areas. In the untransfected surrounding tissues, vessels (**a**) and retinal neurons (**b**) do not express the reporter enzyme (black arrowheads) ( $n = 3$ ). (**c–j**) Localization of  $\beta$ -Galactosidase expression (blue coloration) on paraffin histological sections counterstained (**c–f**) or not (**g–j**) with hematoxylin and eosin in an eye treated by ET using a 40V/cm electrical field intensity (**e,f,h,j**). Comparison was made with an untreated control (**c,g,i**) and an eye treated by ET using an electrical field intensity of 14V/cm (**d**) ( $n = 4$  eyes/group). GCL, ganglion cell layer; INL/ONL, inner/outer nuclear layer; IPL/OPL, inner/outer plexiform layer; IS/OS, photoreceptor inner/outer segments; RPE, retinal pigment epithelium; S, sclera. White, gray, and black arrowheads indicated RPE cells, choriocapillary vessels and choroid vessels, respectively. Black arrowheads in **j** indicated photoreceptors cytoplasm or nucleus. Gene expression is detected in vessels of the choroid and the choriocapillary, in the RPE cell layer, in photoreceptor OS and IS and in the ONL.

Regarding the volume of injection, preliminary experiments had demonstrated that volumes of 30  $\mu$ l (or 40  $\mu$ l) were required to achieve a good transfection efficacy when combined with ET (60 V/cm, 20 ms, 5 Hz) and that smaller volumes like 20  $\mu$ l were less adapted when using the same amount of plasmid (data not shown,  $n = 4$  eyes/group). Using 30  $\mu$ l, the area of suprachoroidal detachment was larger allowing transfection to be more extended and more reproducible. No detectable difference could be observed between all volumes using injection alone (data not shown,  $n = 4$  eyes/group).

### Efficacy of suprachoroidal ET

Low-magnification observation of flat-mounted RPE–choroid–sclera complexes and neuroretinas shows that choroidal cells and vessels have been transfected as well as neuronal tissues (Figure 4a,b) ( $n = 3$ ). Histological sections (Figure 4e) confirmed the  $\beta$ -galactosidase activity in choroidal cells, including choroidal vessels, but also showed activity in RPE cells and in photoreceptors outer and inner segments ( $n = 4$ ). Larger magnification (Figure 4f) confirmed transfection of choroidal vessels, regular transfection of RPE cells and  $\beta$ -galactosidase activity in outer and to a lesser extent in inner segments of the photoreceptors. Using phase contrast analysis of unstained sections, the blue coloration resulting from  $\beta$ -galactosidase activity was better detected in choroidal cells including choroidal vessels, in RPE cells and photoreceptor OS (Figure 4h). Higher magnification performed in the most transfected areas highlighted that  $\beta$ -galactosidase activity was also found in the inner part of photoreceptor cells, *i.e.*, in inner segments as well as around photoreceptor nuclei (Figure 4j), suggesting that photoreceptors were transfected.

To discard any artifact that may arise from enzymatic reaction leakage from the RPE cells during X-Gal staining, immunostaining was performed against the  $\beta$ -galactosidase antigen (see **Supplementary Materials and Methods** online for details). A strong and diffuse labeling was observed in the outer segment region of photoreceptor cells of the injected areas ( $n = 6$ ), whereas only low background was found in photoreceptors OS located in adjacent untransfected areas ( $n = 6$ ) and in untreated control eyes ( $n = 2$ ) (results not shown). However, no positive photoreceptor cell body was observed. No background could be detected on negative controls for which the primary antibody was omitted. Moreover, reporter protein expression was confirmed in RPE cells and in the choriocapillary/choroid.

### Duration of transgene expression

As shown in Figure 5,  $\beta$ -galactosidase activity was maximal on day 7 (first time point tested) when transfection was detected in the whole area corresponding to the area of suprachoroidal detachment (Figure 5a). At this time point, the transfected area extended on one third to one quarter of the posterior segment (Figures 2f and 5a). Then, gene expression decreased over time from day 7 to 4.5 months, both at the intensity level and extent level ( $n = 4$  eyes/time point). Compared to the observations made at day 7, staining was less uniform at day 14 even if still strong (Figure 5b). One month after ET,  $\beta$ -galactosidase activity was faint with most expression following a circular ring, corresponding to the edges of the suprachoroidal detachment bleb (Figure 5c).

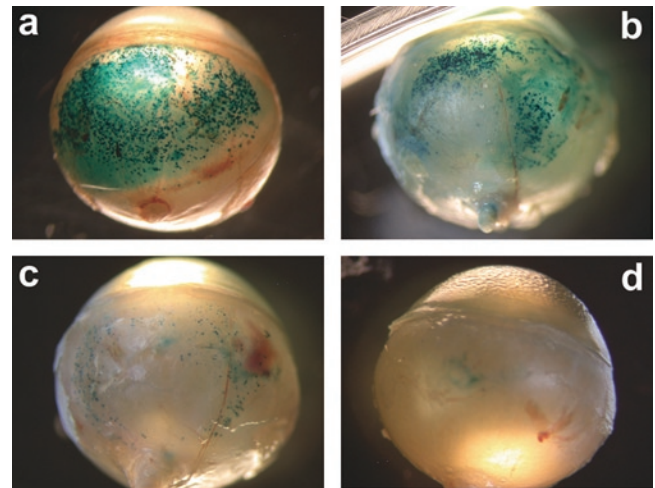


**Figure 5** Time course of transgene expression. Localization and intensity of  $\beta$ -galactosidase expression (blue coloration) observed from outside the eye (a) 7 days, (b) 14 days, (c) 1 month, and (d) 4.5 months after suprachoroidal electrotransfer (40V/cm, 20 ms, 5 Hz; device 2) of pVAX1-LacZ plasmid (30  $\mu$ g in 30  $\mu$ l). Pictures shown are representative of the four eyes analyzed per time point. Transfection efficacy was most prominent at day 7 and decreased over time.

After 4.5 months, reporter gene expression was still detectable only in a restricted area (Figure 5d). Thus, using a cytomegalovirus (CMV) promoter, a significant expression was achieved for at least a month and then decreased until 4.5 months. No pathological changes were noted externally or in eye fundus during the observation period.

### Safety of the procedure

To evaluate the possible changes induced by the suprachoroidal injection and ET procedure on the choroidal and retinal vasculatures, fundi angiographies were performed 3 days after treatment with the plasmid backbone. No vascular leakage or window effects could be observed in the temporal-treated areas (Figure 6b) compared the same area of untreated control eyes (Figure 6a) demonstrating that treatment apparently maintained the integrity of the vessels and RPE ( $n = 8$  eyes/group). Moreover, no leaky vessel could be detected at the optic nerve head level in both groups (Figure 6c,d) suggesting no major early hemoretinal barrier breakdown.

To analyze whether the procedure of suprachoroidal injection and ET had functional consequences on retinal electrophysiology, electroretinographic (ERGs) analyses were recorded 1 week and 7 weeks (7 and 50 days, respectively) after treatment (Figure 6e–j). Over the full range of stimulus intensities tested, no significant long-lasting modifications of scotopic a-wave amplitudes (Figure 6e,h) or latencies (data not shown) could be registered in eyes submitted to suprachoroidal injection of balanced salt solution followed by ET, in comparison to untreated control eyes ( $n = 8$  eyes/group). Indeed, the only statistical decrease in a-wave amplitude observed 1 week after treatment for the stimulus intensity of 0.3 cd.s/m<sup>2</sup> was not maintained after 7 weeks. Moreover, no statistical decrease in scotopic b-wave amplitudes (Figure 6f,i) and latencies (data not shown) were induced by the procedure on both the short- and mid-term, whatever the stimulus intensity considered. Photopic

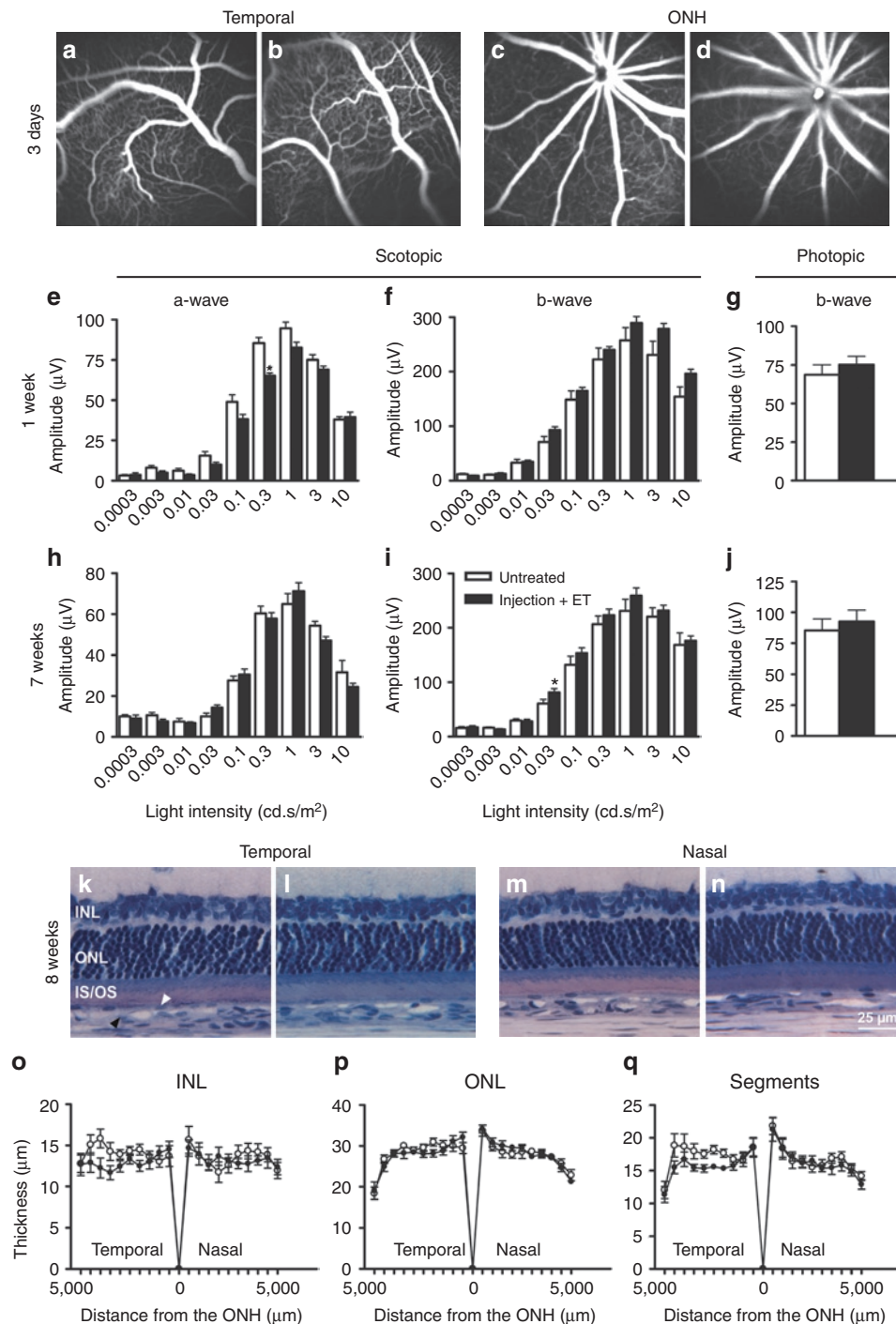


**Figure 6 Short-term and mid-term safety of suprachoroidal electrotransfer.** (a–d) Fluorescein angiographies performed in pigmented Brown-Norway rats 3 days after suprachoroidal injection (30  $\mu$ g, 30  $\mu$ l) and electrotransfer (8 pulses, 40V/cm, 20 ms, 5 Hz; device 2) of noncoding plasmid backbone (b,d). Comparison is made with untreated control eyes (a,c) ( $n = 8$  eyes/group). No vessel leakage is observed in the temporal retina (a,b) or at the optic nerve head (ONH) (c,d) in both groups. (e–j) Scotopic ERG a-wave (e,h) and b-wave (f,i) amplitudes and photopic b-wave (g,j) amplitude recorded one week (e–g) and seven weeks (h–j) after suprachoroidal injection of balanced salt solution (BSS) (30  $\mu$ l) and electrotransfer (8 pulses, 40V/cm, 20 ms, 5 Hz; device 2) in albino Lewis rats ( $n = 8$ ; filled bars). Age-matched untreated eyes were used as negative controls ( $n = 8$ ; open bars). Results are expressed as mean  $\pm$  SEM. Statistical analyses: Mann–Whitney  $U$ -test. \* $P < 0.05$  versus untreated eyes. (k–n) Representative plastic histological sections of retinas 8 weeks after suprachoroidal injection of BSS and electrotransfer (l,n) compared to untreated eyes (k,m). Photos are taken in the injected temporal retina (k,l) and in the contralateral nasal retina (m,n), at 3 mm from the ONH. INL, inner nuclear layer; ONL, outer nuclear layer; IS/OS, photoreceptor inner/outer segments. White and black arrowheads indicated RPE (retinal pigment epithelium) and choriocapillary/choroid vessels respectively. (o–q) INL (o), ONL (p) and photoreceptor segments (IS/OS) (q) thickness profiles along the whole retina in untreated eyes (open circles) and in eyes treated by suprachoroidal injection of BSS and electrotransfer 8 weeks before (filled circles). Thickness measurements were performed every 500  $\mu$ m from the ONH in the temporal and nasal retina and results expressed as mean  $\pm$  SEM for each distance ( $n = 8$  eyes/group). Statistical analysis: Bonferonni test.

b-wave amplitude (Figure 6g,j) and latency (data not shown) were neither statistically different between treated and untreated eyes at the two time points. Representative single ERG recordings, given as **Supplementary Materials and Methods** (see **Supplementary Figure S1**), show that no obvious modification of the amplitude, the latency but also the shape of scotopic a- and b-waves as well as photopic b-wave could be noticed 7 weeks after treatment as compared to untreated control eyes. In addition, no intraocular inflammation could be noticed by slit lamp clinical examination at the same time points.

Histological analyses carried out 8 weeks (56 days) after treatment showed no obvious retinal disorganization or gross structural damage in treated eyes as compared to untreated control ones ( $n = 8$  eyes/group). In the temporal area subjected to both injection and ET, retinal structure was well preserved and the choriocapillary/choroid bed has completely reattached to the retinal pigment epithelium (Figure 6k,l). Morphometric analyses performed along the temporal retina (Figure 6o-q) showed no statistical thinning in the inner nuclear layer, outer nuclear layer or photoreceptor inner/outer segment (IS/OS) between treated and untreated eyes, with mean thicknesses of  $12.9 \pm 0.5 \mu\text{m}$  versus  $14.1 \pm 0.6 \mu\text{m}$  (inner nuclear layer),  $27.8 \pm 0.4 \mu\text{m}$  versus  $28.3 \pm 0.5 \mu\text{m}$  (outer nuclear layer) and  $15.7 \pm 0.3 \mu\text{m}$  versus  $17.3 \pm 0.7 \mu\text{m}$  (IS/OS), respectively. In the nasal hemisphere, only submitted to the electric field, retinal structure was also well preserved (Figure 6m,n) with no significant changes in inner nuclear layer ( $13.3 \pm 0.7 \mu\text{m}$  versus  $13.5 \pm 0.8 \mu\text{m}$ ), outer nuclear layer ( $28.3 \pm 0.4 \mu\text{m}$  versus  $28.1 \pm 0.7 \mu\text{m}$ ) and photoreceptor IS/OS ( $16.4 \pm 0.8 \mu\text{m}$  versus  $16.8 \pm 0.8 \mu\text{m}$ ) thickness between treated and untreated eyes (Figure 6o-q), demonstrating that the selected electric parameters were well tolerated.

### Therapeutic efficacy

The antiangiogenic efficacy of the suprachoroidal ET of a plasmid encoding the rat soluble vascular endothelial growth factor receptor-1 (sFlt-1) was evaluated in a rat model of choroidal neovascularization (CNV). In all groups, no statistical difference in CNV area could be noticed between the temporal and the nasal sides, explaining why all the values measured per eye were averaged into a single one. As shown by observation (Figure 7b-d) and quantification of neovascular areas (Figure 7e) performed at the peak of the disease, a significant reduction of >25% of laser-induced CNV area was observed in rats treated by ET of the therapeutic plasmid ( $18,500 \pm 1,430 \mu\text{m}^2$ ) compared to control eyes treated by ET of the corresponding empty plasmid ( $25,100 \pm 1,710 \mu\text{m}^2$ ) and to untreated control eyes ( $25,700 \pm 1,400 \mu\text{m}^2$ ) ( $n = 8$  eyes/group). Moreover, no exacerbation of CNV could be noticed in pVAX2-treated eyes compared to untreated control eyes.

### DISCUSSION

We have already demonstrated that suprachoroidal administration is a safe and reproducible procedure, allowing the depot of a slow release polymer.<sup>24</sup> Since then, other groups have confirmed the feasibility of this route of administration and particularly the group of T. Olsen who has developed an elegant suprachoroidal catheter equipped with a lighting system to follow the adequate placement of the injector up to the posterior pole and particularly to the macula region.<sup>25</sup> In the present study, we demonstrate that

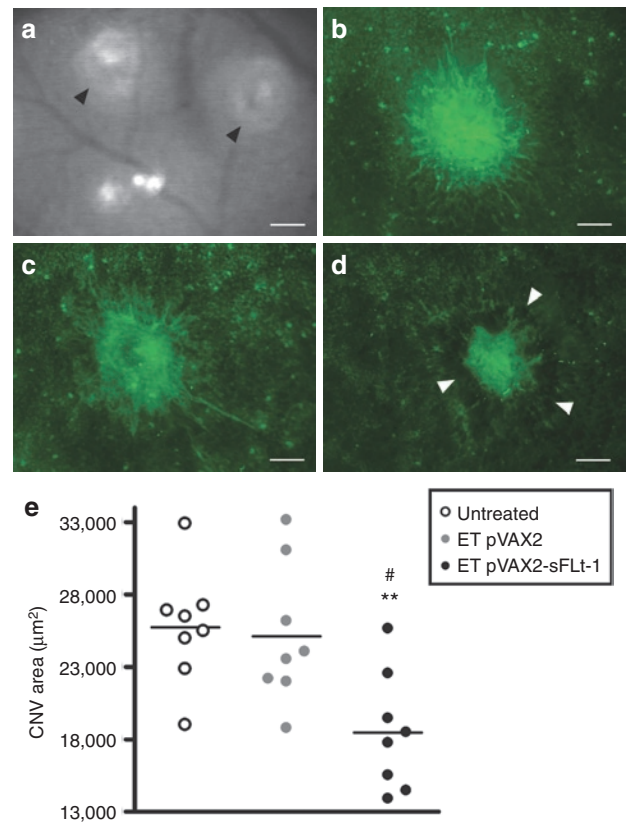


**Figure 7** Therapeutic efficacy of suprachoroidal electrotransfer of a plasmid encoding a vascular endothelial growth factor (VEGF) soluble receptor in a rat model of choroidal neovascularization. (a) Infrared photograph taken immediately after laser argon photocoagulation showing laser impacts (black arrowheads) in the eye fundus. (b-d) Images of choroidal neovascularization (CNV) in retinal pigment epithelial cells (RPE)/choroid/sclera flatmounts labeled with lectin 15 days after laser argon photocoagulation. Images are representative of CNV observed in untreated control eyes (b) and eyes treated by pVAX2 (c) or pVAX2-sFlt-1 (d) suprachoroidal injection and electrotransfer (ET) (8 pulses, 40V/cm, 20ms, 5 Hz; Device 2) 3 days before CNV induction. Bar = 100 $\mu\text{m}$ . White arrowheads indicate the margin of the lesion. (e) Quantification of neovascular areas by digital image analysis performed on RPE/choroid flatmounts showing a significant reduction of CNV in eyes treated by suprachoroidal ET of pVAX2-sFlt-1 compared to untreated control eyes and eyes treated by the empty plasmid (ET pVAX2). In each group, the means of CNV area calculated for each eye (dots;  $n = 8$  eyes/group) were average into a single value (line). Statistical analysis: Mann-Whitney *U*-test. \*\* $P < 0.01$  versus untreated; # $P < 0.05$  versus ET pVAX2.

this route can also be used to deliver plasmid DNA in the choroid and adjacent retinal cells and that the plasmids remained confined in this space longer enough to allow their transduction by *ab externo* application of an ET current. Due to the very high blood flow in the choroid, one could have anticipated that plasmids in a solution would have been washed away within seconds. However, the adequate injection in the suprachoroidal space probably creates a “pocket” in which the plasmid solution is trapped and maintained a pressure on RPE cells for a time sufficient to allow their transfection. How plasmid DNA can reach RPE cells through the Bruch’s membrane is not clear since molecules higher than 300 kDa are not supposed to cross it.<sup>27</sup> However, it was shown that particles in the size range of plasmid, such as lipoprotein particles



of 20–30 nm originating from the retina, were found in the Bruch's membrane.<sup>28</sup> Transfection of adult RPE cells using ET has already been described after subretinal injection of plasmid<sup>29,30</sup> and very recently after suprachoroidal injection of viral vectors.<sup>31</sup> The originality of our work is that we demonstrated here for the first time that transfection of these cells could be efficiently achieved through a nonviral strategy without inducing any surgical detachment of the retina. Contrary to the subretinal approach, choroidal cells were also targeted together with RPE cells, what can be of particular interest to treat diseases affecting both cell types. Similar results have just been published after the suprachoroidal administration of an adeno-associated virus in the rabbit eye.<sup>31</sup> Further studies would thus be required to analyze the transport mechanisms responsible for plasmid diffusion from the suprachoroidal space to the RPE cells and possibly to the neuroretina. The more unexpected observation was that, although the encoded protein did not carry any specific signal peptide, it was preferentially detected in the outer segment region of photoreceptors cells rather than in their whole cellular body, as confirmed both by enzymatic reaction and immunohistochemistry. Since this localization is an unusual observation, further studies will be required to ascertain that photoreceptors are effectively transduced, for example by performing confocal microscopy analyses or immunostaining of dissociated retinal cells. Yet, these results would be consistent with the expression pattern found in these cells after suprachoroidal administration of adeno-associated virus.<sup>31</sup> Interestingly, photoreceptors have not yet been efficiently transfected by electroporation in adult rodents, even when plasmid DNA was injected into the subretinal space.<sup>21</sup> Nevertheless, the detection of  $\beta$ -galactosidase activity in some photoreceptor inner and OS<sup>30</sup> and of rare green fluorescent protein-positive cells in the outer nuclear layer<sup>32</sup> reported after subretinal ET, taken together with our results, suggest the possibility to transduce mature photoreceptors *in vivo* by electroporation. Transfection efficacy could thus be closely related to the shape and placement of the two electrodes as well as to the settings of electric parameters that together determine the distribution and strength of the current field.

In addition to the injection, the electric field is crucial for electroporation to occur as shown by the absence of transfection when the plasmid was injected without current application. The most challenging aspect when using *in vivo* electroporation is that appropriate parameters must be adapted for each tissue to define not only the efficacy but also the toxicity thresholds. In these experiments, transfection efficacy was reached at 40 V/cm (*i.e.*, 20 V) and toxicity was noticed when the current was higher than 120 V/cm (60 V). Even if further studies would be required to define more precisely the retinal toxicity thresholds, we demonstrated that under our selected parameters, suprachoroidal injection followed by ET (40 V/cm) did not induce any burn or inflammatory reaction and apparently maintained the integrity of retinal and choroidal vasculatures as assessed on fluorescein angiography. More importantly, the integrity of retinal structure was not affected correlating well functional data showing that scotopic and photopic retinal electrophysiological responses were similar to those measured in normal eyes. These results are consistent with previous studies showing that suprachoroidal injection was well tolerated,<sup>24</sup> even in the macular region,<sup>25</sup> and that

application of an electric field of 34 V/cm did not induce any adverse effects on retinal morphology or functions in rodents.<sup>30</sup> Thus our results demonstrate that suprachoroidal injection combined with ET could be used even at the posterior pole without major safety concerns what is of course of the utmost importance if the macula should be targeted.

Under the control of the ubiquitous viral CMV promoter, LacZ reporter gene expression was maintained for 15 days after treatment, decreasing rapidly within 1 month. This short-term expression has already been described in RPE cells after subretinal ET in the adult mouse<sup>23</sup> and rat retina,<sup>33</sup> using the same promoter. The transitory gene expression could be attributed to the transcriptional silencing associated with the methylation of the CMV promoter<sup>34</sup> rather than a loss of plasmid DNA in the target cells. Indeed, replacement of viral promoters by RPE-specific mammalian promoters resulted in a sustained expression for several months in RPE cells after subretinal ET in the adult mouse.<sup>23</sup> Moreover, after subretinal delivery of compacted DNA nanoparticles carrying a therapeutic gene in a mouse model of retinal degeneration, functional rescue of rods and cones was more prolonged when using a photoreceptor-specific promoter rather than a viral promoter.<sup>35</sup> Thus, ongoing experiments are evaluating the efficacy of cell-specific promoters to prolong the duration of expression in the target cells after suprachoroidal ET.

The primary attractive technical aspect of our approach is that suprachoroidal administration of vector is efficient to transfect the external retina by avoiding retinal complications that may arise from subretinal injections.<sup>5,6,11</sup> Furthermore, the use of a nonviral gene transfer strategy could alleviate vector-associated complications. As compared to the recently developed suprachoroidal injection of viral vectors, the use of plasmid DNA and electroporation is expected to be safer if the vector is drained from the suprachoroidal space to the bloodstream through the fenestrated choriocapillary. Indeed, naked plasmid DNA do not have the ability to transfect cells, even if released in the systemic circulation, as already demonstrated in clinical trials using plasmid DNA ET in skeletal muscles.<sup>36</sup> Moreover, the use of plasmid DNA could be of particular interest to circumvent the safety concerns arising from the diffusion of viral particles into the brain following intraocular administration of viral vectors.<sup>8</sup> Suprachoroidal electroporation of plasmids could be used to target retinal cells as well as choroidal cells to produce antiangiogenic proteins or peptides *in situ* for the treatment of CNV. As a proof-of-concept, we have used sFlt-1 that efficiently inhibited CNV not only in the treated temporal retina but also in the nasal untreated retina, demonstrating that local diffusion could occur. Other experiments are ongoing to evaluate the real potential of this novel method for the treatment of choroidal and retinal diseases.

This is the first demonstration that an efficacious nonviral gene transfer procedure can be used to transfect not only the choroid, with potential applications for choroidal neovessels targeting, but also RPE cells and potentially photoreceptors. Not only nonviral vectors were used, but a minimally invasive procedure was performed avoiding retinal detachment and any intraocular electrode placement. As this novel technique is still very young and probably perfectible, further technical improvements are ongoing to design a simple disposable device to treat specifically the posterior pole of human size eyes.

## MATERIALS AND METHODS

**Animals.** Eight- to ten-week-old female albino Lewis rats (Elevage Janvier, Le Genest Saint Isle, France) were used in most of the experiments and handled in accordance with the ARVO Statement for the Use of Animals in Ophthalmic and Vision Research. For fluorescein angiography follow-up, 8–10 weeks male pigmented Brown-Norway rats (Charles River, L'Arbresle, France) were used. Rats were anesthetized by intramuscular injection of ketamine (75 mg/kg) (Virbac, Magny-en-Vexin, France) + largactil (0.5 mg/kg) (Sanofi-Aventis, Paris, France). At the end of the experiments, animals were sacrificed by carbon dioxide inhalation.

**Plasmids.** The commercially available pVAX1-LacZ plasmid encoding for the  $\beta$ -galactosidase reporter gene, under the control of a CMV promoter (6 kbp, 25 nm; Invitrogen, Carlsbad, CA) was used to localize gene expression after suprachoroidal injection followed or not by ET. The pVAX2-sFlt-1 plasmid (4.9 kbp), encoding the rat sFlt-1, was constructed after isolation and reverse transcription of the sFlt-1 mRNA extracted from rat placenta followed by amplification and subcloning of the cDNA downstream of the in the CMV  $\beta$ -promoter in the pVAX2 backbone. Its sequence has been checked by DNA sequencing and it has been validated in a rat model of CNV after delivery through ciliary muscle ET (unpublished results). In this study, it was used to evaluate its efficacy through suprachoroidal ET delivery in the same model. The noncoding pVAX1 and pVAX2 plasmids backbone were used as negative controls. Plasmids were amplified in *Escherichia coli* bacteria and prepared endotoxin-free (EndoFree Plamid Kit; Qiagen, Courtabouef, France). Plasmids were diluted in endotoxin-free water containing 77 mmol/l of NaCl (half saline) (saline, NaCl 0.9%, Versol; Laboratoire Aguettant, Lyon, France) as previously described.<sup>26</sup> The concentration of DNA was determined by spectroscopy measurements (optical density at 260 nm).

**Injection of DNA into the suprachoroidal space.** Plasmid DNA (30  $\mu$ g), balanced salt solution for ocular use (Aqsia, Balanced Salt Solution; Bausch & Lomb, Montpellier, France) or Mayer's hemalun solution were injected into the suprachoroidal space using a curved 30G disposable needle (Micro-Fine + Demi syringe, 0.30  $\times$  8 mm; BD Biosciences, Le Pont de Claix, France) and under a volume of 30  $\mu$ l (unless stated otherwise). Injection was performed in the temporal hemisphere of the eye at 1-mm posterior to the limbus (Figure 1a). After perforating the sclera, the needle could be easily visualized in the suprachoroidal space (Figure 1a). Injection was performed slowly to progressively induce opening of this virtual space.

**ET to the suprachoroidal space.** Immediately after injection of plasmid DNA into the suprachoroidal space, the inoculated area was submitted to an electrical field using the device presented in Figure 2d (device 2). A contact curved Pt/Ir sheet (anode, +) was attached to the sclera, just above the injected area (Figure 2e). A semiannular Pt/Ir sheet (cathode, -) was placed on the sclera, facing the anode at the opposing side of the eye (Figure 2e). All electrodes were home made from platine folds purchased from Good Fellow (Lille, France) and the distance between the electrodes was  $\sim$ 0.5 cm. ET was performed by applying 8 square waves electrical pulses [40 V/cm electrical field intensity (*i.e.*, 20 V voltage), 20 ms duration, 5 Hz frequency] generated by the 830 BTX electropulsator (Genetronics, San Diego, CA). This standard procedure (device and electrical parameters) was used in most experiments, except those designed to evaluate other electrical devices or other electrical parameters (see Results section and Figures 2 and 3 for details).

**Eye fundi examinations.** Immediately after suprachoroidal injection, eye fundi were examined under an operating microscope, using a coverslide applied on the corneal surface, to evaluate the accurate placement of the injection and to ensure that no area of retinal detachment has occurred. Photos were taken using a numeric camera (Coolpix; Nikon, Fnac, Paris, France).

Fluorescein angiography was performed on anesthetized pigmented rats 3 days after treatment, before CNV induction (see "Therapeutic

application" section). For this purpose, pupils were dilated with 1% tropicamide and fluorescein (0.2 ml of 10% fluorescein in saline) was administered intravenously. Angiograms were established in the temporal-treated area and at the optic nerve head using a confocal scanning laser ophthalmoscope (HRA; Heidelberg Engineering, Dossenheim, Germany).<sup>37</sup>

**Histological analyses of suprachoroidal detachment and retinal morphology.** For suprachoroidal detachment analysis, eyes were enucleated 2–5 minutes after suprachoroidal injection of Mayer's hemalun solution. For morphometric analysis, eyes were harvested 56 days after suprachoroidal injection of balanced salt solution followed by ET. Freshly enucleated eyes were immediately fixed with a mixture of 4% paraformaldehyde and 0.5% glutaraldehyde in phosphate-buffered saline (PBS) for 2 hours at room temperature. They were rinsed for 2 hours in PBS, dehydrated at room temperature with increasing ethanol concentrations before being incubated overnight at 4 °C with infiltration solution provided in the Leica Histoiresin Embedding kit. Samples were embedded in resin (Leica, Rueil-Malmaison, France) and 5- $\mu$ m thick histological sections passing through the optic nerve head were performed along the nasotemporal plane of the eye using a microtome (Leica). Sections were stuck on gelatin-coated slides, stained for 2 minutes with 1% toluidine blue solution and observed by light microscopy under an Aristoplan light microscope (Leica) coupled with a Leica DFC480 camera.

For morphometric analysis, photographs were made along the whole retina. Thicknesses of inner nuclear layer, outer nuclear layer and photoreceptor inner and OS were measured manually on histological sections using the ImageJ free software (one section per eye). Measurements were performed every 500  $\mu$ m, at a distance of 500–5,000  $\mu$ m from the ONH, in both the temporal and nasal hemispheres. Thickness profiles along the retina were generated by averaging, for each distance, the values obtained for all eyes treated similarly. For each distance, experimental groups were compared using the Bonferonni test. The values obtained for each eye in the temporal and nasal sides were averaged out into a single value corresponding to the mean thickness along the temporal and nasal retina; temporal and nasal values obtained from all eyes belonging to the same experimental group were then averaged and compared using the Mann-Whitney *U*-test.

**$\beta$ -Galactosidase activity visualization.** To localize  $\beta$ -galactosidase gene expression in ocular tissues, eyes were enucleated 7 days, 14 days, 1 month, or 4.5 months after suprachoroidal ET of the pVAX1-LacZ. pVAX1 backbone was used as control. Freshly enucleated eyes were incised at the limbus and fixed for 1 hour at 4 °C in PBS containing 2% paraformaldehyde and 0.2% glutaraldehyde. They were rinsed three times in PBS before being incubated overnight (*i.e.*, 15–16 hours) at room temperature with 1 mg/mL X-gal (5-bromo-4-chloro-3-indolyl galactopyranoside; Sigma-Aldrich, Saint-Quentin Fallavier, France) in PBS containing 5 mmol/l of  $K_3Fe(CN)_6$ , 5 mmol/l of  $K_4Fe(CN)_6$ , 2 mmol/l of  $MgCl_2$  and 0.02% NP40, as detailed previously.<sup>38</sup> After washing with PBS, direct imaging from the outside of the eyes was realized using a numerized camera (Coolpix; Nikon).

Analyses were then carried out on histological sections and flatmounts. For histological analyses, eyeballs were dehydrated at room temperature with increasing ethanol concentrations before being embedded in paraffin. Nasotemporal sections (10- $\mu$ m thick) performed in the blue colored areas expressing the  $\beta$ -galactosidase reporter gene were counterstained with hematoxylin-eosin and observed by light microscopy under an Aristoplan light microscope (Leica) coupled with a Leica DFC480 camera. For flatmount analyses, eyes were carefully dissected by transversal section at 1 mm from the limbus. Anterior segments were discarded and the neuroretinas were carefully separated from the remaining RPE-choroid-sclera complexes. Neuroretinas and RPE-choroid-sclera complexes were flat-mounted separately in PBS/glycerol (1/1, vol/vol) and observed under an operating microscope using a numerized camera (Coolpix; Nikon).

**ERG.** Electroretinographic analyses were performed 7 days and 50 days after treatment (8 eyes per group). For full-field ERG recordings, rats were anesthetized by intramuscular injection (0.8–1.2 ml/kg) of a solution containing ketamine (40 mg/ml; Ketamine 1,000; Virbac, Carros, France) and xylazine (4 mg/ml; Rompun 2%; Bayer Santé, Puteaux, France). The cornea was desensitized with a drop of tetracaine chlorhydrate 1% (Tetracaine; TVM, Lempdes, France) and the pupils were dilated with a drop of Tropicamide (Mydriaticum; Théa, Clermont-Ferrand, France). One drop of hydroxyethylcellulose (Gelaser; Alcon, Fort Worth, TX) was applied to the cornea to keep it hydrated and for electrical conductance. Gold wiring electrodes placed on the corneas of both eyes and electrodes inserted into the forehead served as working electrodes and reference electrodes, respectively. A stainless steel needle electrode was subcutaneously inserted at the base of the animal tail for grounding. All the manipulations were performed under dim red light. The anesthetized rats were placed in a Ganzfeld bowl, on a sliding table. Measurements were performed using the commercial VisioSystem device (Siem Biomedicale, Nimes, France).

For scotopic ERG measurements, animals were dark-adapted overnight. Flash intensities ranged from 0.0003 to 10 cd.s/m<sup>2</sup>. Five flashes per stimulation intensity were applied at a 0.5 Hz frequency, under scotopic conditions, and corresponding responses were averaged. Flash duration was 10 ms (–30 to 0 dB) except for 10 cd.s/m<sup>2</sup> it was 30 ms (0 dB). For photopic recordings, animals were light-adapted for 10 minutes with a rod-suppressing background light of 25 cd/m<sup>2</sup>. A light flash was then applied, the light intensity being 10 cd.s/m<sup>2</sup> (flash duration 79 ms). Amplitudes (in  $\mu$ V) and latencies (in ms) of  $\alpha$ -wave and  $\beta$ -wave were measured and data obtained from each eye belonging to the same experimental group were averaged.

**Therapeutic application.** CNV was induced by laser photocoagulation in Brown-Norway untreated control eyes or in eyes treated 3 days before by temporal suprachoroidal ET of 30  $\mu$ g of pVAX2 or pVAX2-sFlt-1. A 532-nm argon laser (Viridis 532 nm; Quantel Medical, Clermont-Ferrand, France) mounted on a slit lamp (Hagg-Streit, BQ 900) was used throughout. A glass coverslip fulfilled the role of a contact lens during the laser delivery. Eight laser spots (100  $\mu$ m spot size, 0.1 s duration, and 175 mW power) were performed per eye, with four lesions in the temporal retina and 4 lesions in the nasal retina. The reactive bleb observed at the retinal surface after laser delivery was considered as an evidence of the appropriate focusing and as an indication of the rupture of Bruch's membrane. Eyes were enucleated 15 days after CNV induction and immediately fixed for 15 minutes with paraformaldehyde 4% solution in PBS. After washing in PBS, RPE–choroid–sclera complexes were carefully separated from the neuroretinas and postfixed with methanol 100% for 15 minutes at –20 °C. Tissues were rehydrated in PBS containing 1% Triton X-100 and incubated overnight with lectin from *Bandeiraea simplicifolia* conjugated to fluorescein isothiocyanate (Lectin, FITC labeled, from *Bandeiraea simplicifolia*, BS-I, Ref. L9381; Sigma-Aldrich). After washing in PBS, tissues were flat-mounted using gel mount (Biomed, VWR, Fontenay-sous-Bois, France) and observed by fluorescence microscopy using an Olympus BX51 microscope. Photographs were taken using the same exposure times and contrast settings. CNV areas (in  $\mu$ m<sup>2</sup>) were determined by FITC-lectin fluorescence and measured by outlining the margins of the labeled area on flat mounts images using the ImageJ software. The measurements of neovascular area obtained from multiple lesions were averaged into a single value for each eye. Note that CNV induction and CNV area measurements were performed in a masked fashion by an ophthalmologist and an observer, respectively, who were both unaware of the control and treatment groups.

**Statistical analysis.** For each experiment, the number of eyes (*n*) treated per condition was written in the legend of the figures as well as in the results section. For numerical data, results were expressed as means  $\pm$  SEM and compared using the nonparametric Mann–Whitney *U*-test (Prism 4.0;

Graph Pad Software, San Diego, CA), unless stated otherwise. *P* < 0.05 was considered significant.

## SUPPLEMENTARY MATERIAL

**Figure S1.** Representative single full-field ERG recordings 7 weeks after suprachoroidal electrotransfer.

## Materials and Methods.

## ACKNOWLEDGMENTS

This work was funded in part by the Fondation pour la Recherche Médicale (FRM). This work was done in Paris, France. The authors declared no conflict of interest.

## REFERENCES

- Hamel, C (2006). Retinitis pigmentosa. *Orphanet J Rare Dis* **1**: 40.
- Acland, GM, Aguirre, GD, Ray, J, Zhang, Q, Aleman, TS, Cideciyan, AV *et al.* (2001). Gene therapy restores vision in a canine model of childhood blindness. *Nat Genet* **28**: 92–95.
- Acland, GM, Aguirre, GD, Bennett, J, Aleman, TS, Cideciyan, AV, Bencicelli, J *et al.* (2005). Long-term restoration of rod and cone vision by single dose rAAV-mediated gene transfer to the retina in a canine model of childhood blindness. *Mol Ther* **12**: 1072–1082.
- Bainbridge, JW, Smith, AJ, Barker, SS, Robbie, S, Henderson, R, Balaggan, K *et al.* (2008). Effect of gene therapy on visual function in Leber's congenital amaurosis. *N Engl J Med* **358**: 2231–2239.
- Hauswirth, WW, Aleman, TS, Kaushal, S, Cideciyan, AV, Schwartz, SB, Wang, L *et al.* (2008). Treatment of leber congenital amaurosis due to RPE65 mutations by ocular subretinal injection of adeno-associated virus gene vector: short-term results of a phase I trial. *Hum Gene Ther* **19**: 979–990.
- Maguire, AM, Simonelli, F, Pierce, EA, Pugh, EN Jr, Mingozzi, F, Bencicelli, J *et al.* (2008). Safety and efficacy of gene transfer for Leber's congenital amaurosis. *N Engl J Med* **358**: 2240–2248.
- Romano, G (2009). An update on gene therapy programs. *Drug News Perspect* **22**: 435–440.
- Provost, N, Le Meur, G, Weber, M, Mendes-Madeira, A, Povedin, G, Cherel, Y *et al.* (2005). Biodistribution of rAAV vectors following intraocular administration: evidence for the presence and persistence of vector DNA in the optic nerve and in the brain. *Mol Ther* **11**: 275–283.
- Le Meur, G, Stieger, K, Smith, AJ, Weber, M, Deschamps, JY, Nivard, D *et al.* (2007). Restoration of vision in RPE65-deficient Briard dogs using an AAV serotype 4 vector that specifically targets the retinal pigmented epithelium. *Gene Ther* **14**: 292–303.
- Stieger, K, Schroeder, J, Provost, N, Mendes-Madeira, A, Belbellaa, B, Le Meur, G *et al.* (2009). Detection of intact rAAV particles up to 6 years after successful gene transfer in the retina of dogs and primates. *Mol Ther* **17**: 516–523.
- Jacobson, SG, Boye, SL, Aleman, TS, Conlon, TJ, Zeiss, CJ, Roman, AJ *et al.* (2006). Safety in nonhuman primates of ocular AAV2-RPE65, a candidate treatment for blindness in Leber congenital amaurosis. *Hum Gene Ther* **17**: 845–858.
- Eandi, CM, Chung, JE, Cardillo-Piccolino, F and Spaide, RF (2005). Optical coherence tomography in unilateral resolved central serous chorioretinopathy. *Retina (Philadelphia, Pa)* **25**: 417–421.
- Wilkinson, CP (2009). Mysteries regarding the surgically reattached retina. *Trans Am Ophthalmol Soc* **107**: 55–57.
- Andrieu-Soler, C, Bejjani, RA, de Bizemont, T, Normand, N, BenEzra, D and Behar-Cohen, F (2006). Ocular gene therapy: a review of nonviral strategies. *Mol Vis* **12**: 1334–1347.
- Bejjani, RA, Andrieu, C, Bloquel, C, Berdugo, M, BenEzra, D and Behar-Cohen, F (2007). Electrically assisted ocular gene therapy. *Surv Ophthalmol* **52**: 196–208.
- Bloquel, C, Bourges, JL, Touchard, E, Berdugo, M, BenEzra, D and Behar-Cohen, F (2006). Non-viral ocular gene therapy: potential ocular therapeutic avenues. *Adv Drug Deliv Rev* **58**: 1224–1242.
- Mir, LM, Moller, PH, André, F and Gehl, J (2005). Electric pulse-mediated gene delivery to various animal tissues. *Adv Genet* **54**: 83–114.
- Mir, LM (2008). Application of electroporation gene therapy: past, current, and future. *Methods Mol Biol* **423**: 3–17.
- Isaka, Y and Imai, E (2007). Electroporation-mediated gene therapy. *Expert Opin Drug Deliv* **4**: 561–571.
- Daud, AI, DeConti, RC, Andrews, S, Urbas, P, Riker, AI, Sondak, VK *et al.* (2008). Phase I trial of interleukin-12 plasmid electroporation in patients with metastatic melanoma. *J Clin Oncol* **26**: 5896–5903.
- Matsuda, T and Cepko, CL (2004). Electroporation and RNA interference in the rodent retina *in vivo* and *in vitro*. *Proc Natl Acad Sci USA* **101**: 16–22.
- Chen, B and Cepko, CL (2009). HDAC4 regulates neuronal survival in normal and diseased retinas. *Science* **323**: 256–259.
- Kachi, S, Esumi, N, Zack, DJ and Campochiaro, PA (2006). Sustained expression after nonviral ocular gene transfer using mammalian promoters. *Gene Ther* **13**: 798–804.
- Einmahl, S, Savoldelli, M, D'Hermies, F, Tabatabay, C, Gurny, R and Behar-Cohen, F (2002). Evaluation of a novel biomaterial in the suprachoroidal space of the rabbit eye. *Invest Ophthalmol Vis Sci* **43**: 1533–1539.
- Olsen, TW, Feng, X, Wabner, K, Conston, SR, Sierra, DH, Folden, DV *et al.* (2006). Cannulation of the suprachoroidal space: a novel drug delivery methodology to the posterior segment. *Am J Ophthalmol* **142**: 777–787.
- Touchard, E, Kowalczyk, L, Bloquel, C, Naud, MC, Bigey, P and Behar-Cohen, F (2010). The ciliary smooth muscle electrotransfer: basic principles and potential for sustained intraocular production of therapeutic proteins. *J Gene Med* **12**: 904–919.

27. Hussain, AA, Starita, C, Hodgetts, A and Marshall, J (2010). Macromolecular diffusion characteristics of ageing human Bruch's membrane: implications for age-related macular degeneration (AMD). *Exp Eye Res* **90**: 703–710.
28. Wang, L, Li, CM, Rudolf, M, Belyaeva, OV, Chung, BH, Messinger, JD *et al.* (2009). Lipoprotein particles of intraocular origin in human Bruch membrane: an unusual lipid profile. *Invest Ophthalmol Vis Sci* **50**: 870–877.
29. Johnson, CJ, Berglin, L, Chrenek, MA, Redmond, TM, Boatright, JH and Nickerson, JM (2008). Technical brief: subretinal injection and electroporation into adult mouse eyes. *Mol Vis* **14**: 2211–2226.
30. Kachi, S, Oshima, Y, Esumi, N, Kachi, M, Rogers, B, Zack, DJ *et al.* (2005). Nonviral ocular gene transfer. *Gene Ther* **12**: 843–851.
31. Peden, MC, Min, J, Meyers, C, Lukowski, Z, Li, Q, Boye, SL *et al.* (2011). Ab-externo AAV-mediated gene delivery to the suprachoroidal space using a 250 micron flexible microcatheter. *PLoS ONE* **6**: e17140.
32. Zhang, M, Mo, X, Fang, Y, Guo, W, Wu, J, Zhang, S *et al.* (2009). Rescue of photoreceptors by BDNF gene transfer using *in vivo* electroporation in the RCS rat of retinitis pigmentosa. *Curr Eye Res* **34**: 791–799.
33. Chalberg, TW, Genise, HL, Vollrath, D and Calos, MP (2005). phiC31 integrase confers genomic integration and long-term transgene expression in rat retina. *Invest Ophthalmol Vis Sci* **46**: 2140–2146.
34. Brooks, AR, Harkins, RN, Wang, P, Qian, HS, Liu, P and Rubanyi, GM (2004). Transcriptional silencing is associated with extensive methylation of the CMV promoter following adenoviral gene delivery to muscle. *J Gene Med* **6**: 395–404.
35. Cai, X, Nash, Z, Conley, SM, Fliesler, SJ, Cooper, MJ and Naash, MI (2009). A partial structural and functional rescue of a retinitis pigmentosa model with compacted DNA nanoparticles. *PLoS ONE* **4**: e5290.
36. Low, L, Mander, A, McCann, K, Dearnaley, D, Tjelle, T, Mathiesen, I *et al.* (2009). DNA vaccination with electroporation induces increased antibody responses in patients with prostate cancer. *Hum Gene Ther* **20**: 1269–1278.
37. Paques, M, Simonutti, M, Roux, MJ, Picaud, S, Levavasseur, E, Bellman, C *et al.* (2006). High resolution fundus imaging by confocal scanning laser ophthalmoscopy in the mouse. *Vision Res* **46**: 1336–1345.
38. Touchard, E, Bloquel, C, Bigey, P, Kowalczyk, L, Kowalczyk, L, Jonet, L *et al.* (2009). Effects of ciliary muscle plasmid electrotransfer of TNF-alpha soluble receptor variants in experimental uveitis. *Gene Ther* **16**: 862–873.